International Journal of Greenhouse Gas Control 53 (2016) 274–283

Contents lists available at ScienceDirect

International Journal of Greenhouse Gas Control

journal homepage: www.elsevier.com/locate/ijggc

Three-dimensional structure of natural convection in a porous medium: Effect of dispersion on finger structure

Lei Wang*, Yuji Nakanishi, Akimitsu Hyodo, Tetsuya Suekane

Department of Energy Sciences, Tokyo Institute of Technology, 4259-G3-31, Nagatsuta, Midori-ku, Yokohama 226-8502, Japan

ARTICLE INFO

Article history:
Received 26 May 2016
Received in revised form 16 August 2016
Accepted 17 August 2016

Keywords:
Natural convection
Three-dimensional images
X-ray computed tomography
Transverse dispersion
Fingering structure

ABSTRACT

Density-driven natural convection in a porous medium is of great interest in the geoscience and geoengineering fields, especially for carbon dioxide capture and storage (CCS). In this study, we applied a novel experimental approach to three-dimensional (3D) imaging of density-driven natural convection in a porous medium. Miscible fluid pairs with nonlinear density properties (a sodium chloride solution and a mixture of methanol and ethylene glycol doped with sodium iodide) were used to model density-driven natural convection from 3D imaging captured by X-ray computed tomography (CT). Slight fluctuations that appeared at the interface grew into large "fingers," which interacted and merged with the neighboring fingers. The fingers extended vertically downward without changing their locations, forming a columnar structure. The finger-extension velocity increased in line with the Rayleigh number and was correlated with the characteristic velocity. The 3D images captured the local concentration of fingers in the course of convective mixing. We found that the decrease in finger-number density was not only related to the Rayleigh number but was also affected by transverse dispersion between the downward- and upward-flow regions. There was an exponential relationship between the finger-number density and the transverse dispersion coefficient. Transverse dispersion caused broadening of the fingers and reduction in the finger-number density because of the interaction and merging of fingers. In carbon dioxide (CO_2) geological storage applications, this transverse dispersion influences the long-term-dissolution process of CO_2 injected into aquifers.

1. Introduction

Carbon dioxide (CO_2) capture and storage (CCS) is one approach to mitigate greenhouse gases in the atmosphere. The injection of CO_2 into saline (brine) formations has received renewed attention because of its capacity to sequester large amounts of CO_2 and reduce climate change.

Under typical reservoir conditions, CO_2 is in a supercritical state with a density less than that of brine. To overcome CO_2 buoyancy and allow CO_2 to be trapped in reservoirs, four mechanisms (Huppert and Neufeld, 2014) are considered: (1) structural and stratigraphic trapping by an impermeable layer; (2) capillary trapping in narrow pore spaces, preventing CO_2 from moving upward (Bandara et al., 2011; Chaudhary et al., 2013; Iglauer et al., 2011; Jiang and Tsuji, 2016; Li et al., 2014; Pentland et al., 2011; Taku Ide et al., 2007; Suekane et al., 2008); (3) dissolution trapping in brine formations (Gilfillan et al., 2009; Iglauer, 2011; Lindeberg and Wessel-Berg, 1997; Lindeberg and Bergmo, 2003; Riaz and Cinar, 2014); and (4) mineral trapping (Gaus, 2010; Klein et al., 2013; Strazisar et al., 2006). In the early stages of CO_2 storage, i.e., during and shortly after injection, a large CO_2 plume may float upwards because of its buoyancy and accumulate beneath an impermeable layer. A major concern of CCS, therefore, is the potential risk of CO_2 leakage, which is expected to have a negative impact on the surrounding environment and on subsoil microbes. Dissolution of CO_2 into brine formations considerably improves the security of storage, because CO_2 dissolved in brine is no longer buoyant. Key outstanding questions are the mechanism and rate of CO_2 dissolution into brine.

When CO_2 is injected into a reservoir, it reaches supercriticality at a depth of 1–3 km beneath the Earth's surface. Supercritical CO_2 with a density of 600–700 kg/m^3 (lighter than ambient groundwater) will rise until it encounters an impermeable rock (Arts et al., 2008), becoming structurally trapped beneath it. In the course of this migration, some fraction of the CO_2 separates from the CO_2 plume and is trapped in porous rocks by capillary force. The CO_2 then dissolves into brine, but the thickness of the CO_2-saturated brine layer is limited because of the very slow rate of diffusion of

---

* Corresponding author.
E-mail address: wang.l.ah@m.titech.ac.jp (L. Wang).

http://dx.doi.org/10.1016/j.ijggc.2016.08.018
1750-5836/© 2016 Elsevier Ltd. All rights reserved.

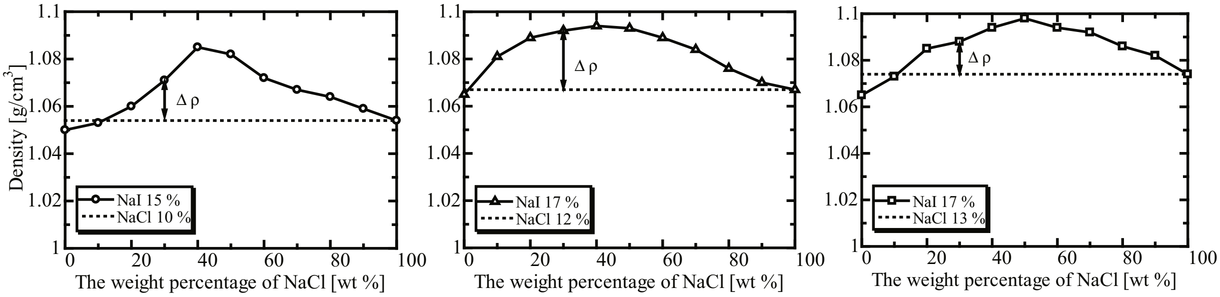

Fig. 1. Density profiles of the mixture of MEG-NaI and NaCl at NaCl concentrations of (a) 10, (b) 12, and (c) 13 wt%. The representative density difference ($\Delta\rho$) between MEG-NaI and NaCl solution was defined at NaCl concentrations of 30 wt%.

CO_2 molecules in brine. Since CO_2-saturated brine is 1–2% denser than groundwater (Yang and Gu, 2006), depending on its CO_2 concentration, instability is induced between the miscible CO_2-saturated brine and CO_2-free brine. The density increase produces a convective flow in which heavier CO_2-saturated brine sinks downward, while lighter CO_2-free brine floats upward in the form of convective fingers. This accelerates CO_2 dissolution and provides a more secure mechanism for CO_2 storage. Thus, density-driven natural convection is induced on a reservoir scale. Natural convection governs the rate of CO_2 mass transfer into the brine, significantly impacting the deep carbon cycle that governs the long-term fate of CO_2 in geological storage.

In North Sea reservoirs, Rayleigh number is very large, at $Ra \sim 10^3$–10^4 (Lindeberg and Wessel-Berg, 1997; Neufeld et al., 2010; Xu et al., 2006). The onset of natural convection and the mass transport of dissolved CO_2 molecules significantly impact the long-term behavior of CO_2 injected into geological formations. The convection process has been investigated using numerical simulations (Chevalier et al., 2014; Ennis-King and Paterson, 2003; Ghesmat et al., 2010; Hidalgo and Carrera, 2009; Xie et al., 2011). Recent improvements in computed performance have facilitated three-dimensional (3D) numerical simulations at high Ra in the presence of flat finger structures (Pau et al., 2010) and strong scaling of the wavenumber (Hewitt et al., 2014), which are particular to 3D natural convection. Experimental studies have also been conducted using two-dimensional (2D) porous media (Cooper et al., 2014; MacMinn et al., 2012; Touvet et al., 2011), including Hele–Shaw cells (Ehyaei and Kiger, 2014; Faisal et al., 2013, 2015; Slim et al., 2013), because of the opaque property of porous materials, but not magnetic resonance imaging (MRI) (Johannsen et al., 2006). To model density-driven natural convection, the nonlinear density profile of a mixture of miscible fluids, of which the details are to be mentioned later, has been used in a number of 2D experimental studies (Backhaus et al., 2011; Huppert et al., 1986; Neufeld et al., 2010).

In this study, we introduced a novel experimental analogue fluid model that allows 3D imaging of the development of density-driven natural convection in a porous medium using X-ray CT. A mixture of miscible fluids, in this case methanol and ethylene-glycol (MEG) doped with sodium iodide (MEG-NaI) and a sodium chloride (NaCl) solution, exhibits a nonlinear density profile, such that its density is higher than that of pure fluid. In this paper, we first present the experimental analogue fluid model, then discuss the 3D structure of the extending fingers that are associated with density-driven natural convection. 3D imaging was used to provide the local concentration in the fingers, which is critical when analyzing the effect of Taylor dispersion on the structure of the fingers. Our investigation of the effect of transverse dispersion on the finger structure provides insights into both the mixing mechanism and the long-term fate of CO_2 injected into deep saline aquifers.

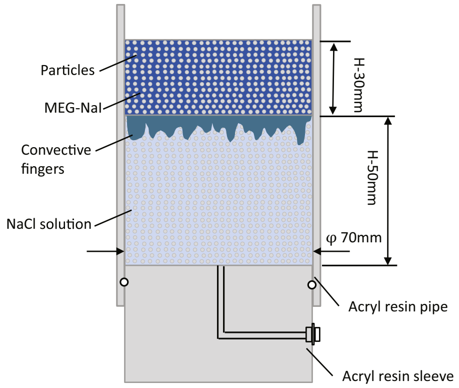

Fig. 2. Packed bed of melamine resin particles.

2. Experimental method

Neufeld et al. (2010) utilized the nonlinearity of the density between a mixture of MEG and water to conduct a 2D experimental study of density-driven natural convection. We expanded this to three-dimensions by doping the fluids with NaI and/or NaCl, allowing visualization with an X-ray CT scanner. Because the salts are highly soluble in each phase, the density contrast and the X-ray attenuation contrast can be controlled by adjusting the doping concentration. After trials of several pairings of concentrations, we determined that the concentrations shown in Fig. 1 are best for modeling the conditions at high Rayleigh numbers $Ra = (Hkg\Delta r)/(\varphi D_m \mu)$, where H is the characteristic macroscopic length, which we defined as the height of the packed bed (80 mm in Fig. 2) and held constant throughout the experiments, k is the permeability, g is the gravitational acceleration $\Delta\rho$ is the density difference between the mixture of MEG-NaI and NaCl solutions and the NaCl solution, φ is the porosity, D_m is a molecular diffusion coefficient, and μ is the viscosity of the NaCl solution. The molecular diffusion coefficient of iodide ions in water depends on both temperature and concentration (Wang and Kennedy, 1950). In the present study, we used a constant value of 2×10^{-9} m^2/s.

Before mixing, the MEG-NaI is less dense than the NaCl solution. However, the density of the mixture exceeds that of the NaCl solution, to a degree that depends on the fraction of MEG-NaI, as shown in Fig. 1. The increase in density causes an unstable stratification that drives natural convection, forming descending fingers. A representative density difference defined at 70 wt% of MEG-NaI, denoted with arrows in Fig. 1, was used to evaluate the Ra, since the weight percentage of MEG-NaI in the fingers that formed at the interface ranged from 64 to 72 wt%.

Since the detailed experimental setup has already been presented in Wang et al. (2016), we only briefly describe the experimental procedures and conditions.